Evidence of dynamic crossover phenomena in water and other glass-forming liquids: experiments, MD simulations and theory

2009 J. Phys.: Condens. Matter 21 504102

(http://iopscience.iop.org/0953-8984/21/50/504102)

IOP Publishing Journal of Physics: Condensed Matter

J. Phys.: Condens. Matter **21** (2009) 504102 (11pp) doi:10.1088/0953-8984/21/50/504102

Evidence of dynamic crossover phenomena in water and other glass-forming liquids: experiments, MD simulations and theory

S H Chen[1,5], Y Zhang[1], M Lagi[1,2], S H Chong[3], P Baglioni[2] and F Mallamace[4]

[1] Department of Nuclear Science and Engineering, Massachusetts Institute of Technology, Cambridge, MA 02139, USA
[2] Department of Chemistry and CSGI, University of Florence, Sesto Fiorentino, I-50019 Florence, Italy
[3] Institute for Molecular Science, Okazaki 444-8585, Japan
[4] Dipartimento di Fisica, Università di Messina and IRCCS Neurolesi 'Bonino-Pulejo', I-98166 Messina, Italy

E-mail: sowhsin@mit.edu

Received 22 April 2009, in final form 28 May 2009
Published 23 November 2009
Online at stacks.iop.org/JPhysCM/21/504102

Abstract

In a recent quasi-elastic neutron scattering experiment on water confined in a Portland cement paste, we find that this 3D confined water shows a dynamic crossover phenomenon at $T_L = 227 \pm 5$ K. The DSC heat-flow scan upon cooling and an independent measurement of specific heat at constant pressure of confined water in silica gel show a prominent peak at the same temperature. We show in this paper that this type of behavior is common to many other glassy liquids, which also show the crossover temperature in coincidence with the temperature of a small specific heat peak. We also demonstrate with MD simulations that the dynamic crossover phenomenon in confined water is an intrinsic property of bulk water, and is not due to the confinement effect. Recently, an extended version of the mode coupling theory (MCT) including the hopping effect was developed. This theory shows that, instead of a structural arrest transition at T_C predicted by the idealized MCT, a fragile-to-strong dynamic crossover phenomenon takes place instead at T_C, confirming both the experimental and the numerical results. The coherent and incoherent α relaxation times can be scaled with the calculated viscosity, showing the same crossover phenomenon. We thus demonstrated with experiments, simulations and theory that a genuine change of dynamical behavior of both water and many glassy liquids happens at the crossover temperature T_L, which is 10–30% higher than the calorimetric glass transition temperature T_g.

(Some figures in this article are in colour only in the electronic version)

1. Introduction

The study of the structure and dynamics of supercooled water is one of the most exciting topics in liquid state physics over the last decade [1, 2]. During this period, an innovative method has been devised to allow the study of deeply supercooled water in nanoconfinement [3–9]. For example, when confined in MCM-41 mesoporous silica with inner diameters less than 20 Å, water can be supercooled below the homogeneous nucleation temperature, $T_H = 235$ K. This allows an experimental investigation of the confined water in the region of the bulk water phase diagram normally inaccessible to experimentation because of the inevitable crystallization into hexagonal ice. The relevance of this approach lies in the fact that it is believed that the origin of many anomalies of the water behavior, e.g. the apparent divergence of both the thermodynamic response functions and the transport properties at 228 K, can

[5] Author to whom any correspondence should be addressed.

be attributed to the existence of a second critical point of water, which lies in this range of temperatures but at an elevated pressure [1, 10, 11].

By performing quasi-elastic neutron scattering (QENS) experiments on water confined in MCM-41-S (1D confined water) with a pore diameter of 15 Å, we have been able to investigate the single-particle dynamics of water molecules and to identify a well-defined dynamic crossover phenomenon at ambient pressure at $T_L = 225 \pm 5$ K [6]. Moreover, by following the crossover temperature T_L as a function of pressure and observing the disappearance of the crossover phenomenon above a certain pressure, we were able to estimate the phase point of the possible second liquid–liquid critical point of water at $P_C = 1550 \pm 50$ bar and $T_C = 200 \pm 5$ K [7].

Similar dynamic crossover phenomena have also been reported for surface water (2D confined water) hydrating metal oxide surfaces [12], and biological molecules, such as lysozyme [13], DNA [14] and RNA [15]. Water can also be confined in aged cement pastes (3D confined water) and an analogous crossover is observed around $T_L = 227 \pm 5$ K [16].

More recently, new experimental results have been reported for the study of water confined in single- and double-walled carbon nanotubes (SWNT, DWNT) [17–19], both a 1D host, which have hydrophobic surfaces. It has been shown that in such hosts water dynamics can be explained in terms of a significantly anharmonic water–substrate potential [17]. As far as the α relaxation time of the confined water is concerned, for these cases the dynamic crossover from a non-Arrhenius to an Arrhenius behavior takes place at somewhat lower temperatures.

In all the above-mentioned cases, water is confined in 1D, 2D or 3D environments. It is then natural to ask whether such a crossover phenomenon is only observable in confined water, namely if a confinement effect could give rise to these phenomena. In this regard, we have recently shown by means of MD simulations, where bulk water does not have time to freeze, that a crossover phenomenon in the α relaxation time and the diffusion constant is also observable in a model TIP4P-Ew bulk water system [16], and thus it is an intrinsic property of water.

In this paper we shall demonstrate by quoting the existing experimental data, by a bulk water MD simulation and by an extended version of the mode coupling theory that the dynamic crossover phenomena in both water and common glass-forming liquids are fragile-to-strong crossover phenomena (FSC), which are intrinsic properties of bulk liquid systems and not a peculiar effect due to the confinement [42, 43]. Furthermore, the FSC temperature T_L is about 20% higher than the traditionally emphasized calorimetric glass transition temperature T_g and it is an important transition temperature (or crossover temperature) for the liquid dynamic behavior.

2. Experiments on confined water

Among all the experiments we performed on confined water during the past several years, we shall single out the case of water confined in an aged cement paste (three-dimensional confined water) with a water/dry powder mass ratio equal to 0.4, to highlight the close relationship between the dynamics and the thermodynamics of supercooled water.

Differential scanning calorimetry measurements (DSC) and near-infrared (NIR) spectra confirm that, after eight days from mixing water with cement powder, all the water in the sample is confined in the developing calcium silicate hydrate (C–S–H) gel [20] and the NIR crystallization peak (due to the formation of hexagonal ice) disappears, confirming the inhibition of the crystallization in this nanoconfined water [16, 21]. The state-of-the-art high-resolution Backscattering Spectrometer BASIS at the Spallation Neutron Source (SNS) at the Oak Ridge National Laboratory (ORNL) was then used to measure the broadening of the quasi-elastic peak of the hydrogen atom dynamic structure factor $S_H(Q, E)$. Using incident neutrons of 2.08 meV, BASIS is capable of measuring a dynamic range as large as ± 100 μeV with an elastic energy resolution of 3 μeV (FWHM). In this experiment, both an eight-day-old H_2O hydrated sample and a dry sample of cement powder were measured. The scattering from the dry sample was rather small due to the absence of hydrogen atoms, and thus was subtracted out as a background from the wet sample. The measured QENS spectrum was analyzed with the relaxing cage model (RCM) [22], which has been tested extensively by MD simulations [22, 23] and QENS experiments [6, 7, 13–16]. The results of the analysis are shown in figure 1. This figure intends to show that, if we define the crossover temperature to be the maximum of the slope in the Arrhenius plot of the translational relaxation time ($T_L = 227 \pm 5$ K), which is suggested by the extended MCT to be shown in figure 11 in section 5, the temperature is in coincidence with the peak position of the DSC cooling scan. Thus, the change of slope in the Arrhenius plot (middle panel) is closely related to the peak in specific heat at constant pressure. This is in agreement with the Adam–Gibbs theory [24], which relates the temperature dependence of the structural relaxation time to the change in the configurational entropy of the system. As a result, a specific heat peak at a certain temperature would imply that there is an abrupt change of slope in the Arrhenius plot of the transport property or the associated relaxation time at that same temperature.

In figure 2, we quote the data by Maruyama *et al* which is a genuine specific heat measured at constant pressure for water confined in silica gel of pore size ~30 Å, a 3D confined water similar to hydration water in cement. This is a rather large peak in specific heat with a value of 1.53 cal K^{-1} g^{-1}. It is reassuring to see that the position of the peak is at exactly 227 K, the same as in the cement hydration water case.

3. Experiments on bulk glassy liquids

We would like to show next that the existing data on the transport coefficients of common bulk glassy liquids also exhibit the FSC phenomena. We shall only use four common organic liquids as typical examples here. A more extensive tabulation of transport coefficient data for 88 glass-forming liquids will be presented in a forthcoming paper [26].

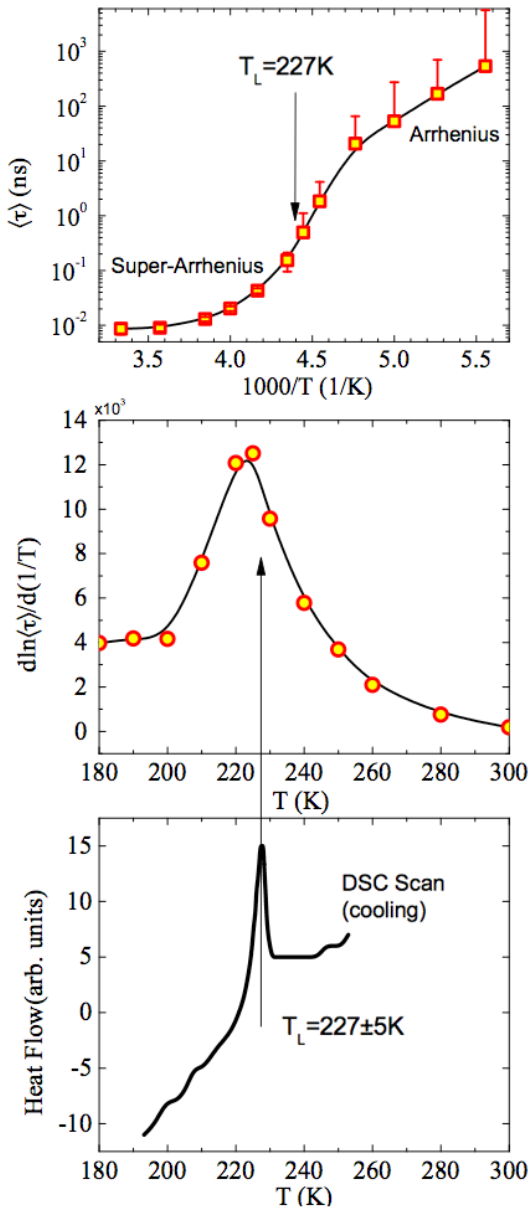

Figure 1. The crossover phenomenon of water confined in aged Portland cement paste [16]. (Top) Arrhenius plot of the α relaxation time extracted by QENS data analysis; (middle) the slope of the Arrhenius plot, showing a peak at the crossover temperature T_L, which is coincident with the heat-flow peak of the DSC cooling scan; (bottom) DSC heat-flow curve of the cooling scan.

Figure 3 shows the Arrhenius plot of the viscosities of o-terphenyl, salol, alpha-phenyl-o-cresol and tri-alpha-naphtylbenzene as measured by Laughlin and Uhlmann [27]. All the plots show a FSC phenomenon because at higher temperatures all four viscosities show a super-Arrhenius behavior (which can be fitted by a Vogler–Fulcher–Tamman law, as indicated by the pink dashed lines). At low enough temperatures, one can see that they all switch to an Arrhenius law which they will follow all the way to the glass transition temperature T_g.

In the insets in the first three panels we also quote the measured specific heat at constant pressure, given by the same

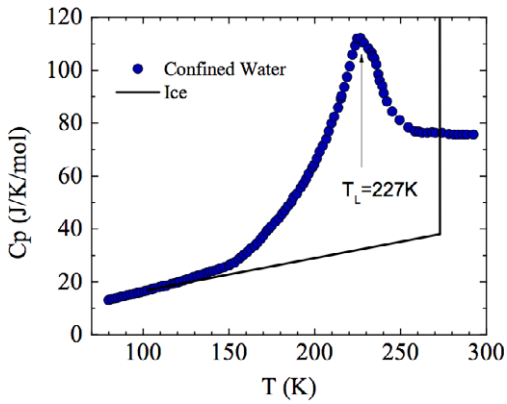

Figure 2. The substantial heat capacity peak of supercooled water confined within pores of silica gel [25]. The pore size is around 3 nm. Note that the peak position is at $T_L = 227$ K, identical to the one in the DSC cooling scan in figure 1.

authors. Note that, compared to the previously shown specific heat in supercooled water (see figure 2), these peaks in organic liquids are rather small (of the order of 0.4 Cal g^{-1}). If we define T_x as the temperature of the peak of the specific heat, then the arrow signs in the main panels confirm, within the error bars, the coincidence with the FSC temperature T_L of the viscosity, namely $T_x = T_L$. Here we may define the FSC temperature T_L as the temperature where the Arrhenius plot of the viscosity has the maximum slope (see figure 11 bottom panel).

In figure 4 we single out the case of o-terphenyl and show the Arrhenius plots of the inverse of the self-diffusion constant (top panel) [28] together with the viscosity (middle panel) and followed by the specific heat (lower panel). It should be noted that the crossover temperatures as indicated by $1/D$ and the viscosity are quite close to each other and agree with the peak position of the specific heat. Again, we confirm the validity of the Adam–Gibbs theory in the case of general organic glass-forming liquids. One consequence of the Adam–Gibbs theory [24] is that, if the specific heat shows a peak at a certain temperature T_x, then the viscosity or the relaxation time will show a change of slope at the temperature of the peak.

4. Computer simulations on bulk water

To make sure that these phenomena are inherent properties of water and not due to the confinement, we ran a simulation of a model bulk water, TIP4P-Ew [29]. Our choice of this specific water model is justified by the excellent agreement of its calculated diffusion constant with the experimental values for bulk water over a wide range of temperatures (between 240 and 320 K). The dynamic crossover in the Arrhenius plot of the self-diffusion constant has been previously observed with simulations of bulk water using other water models [30, 31]. We calculated long MD trajectories for a box of 512 water molecules of up to 1 μs in the *NVT* ensemble. The systems were considered equilibrated when the mean square displacement of the water molecules was larger than 0.1 nm^2 [32] (see the inset of figure 5, bottom right panel). The results of the simulation are shown in figure 5.

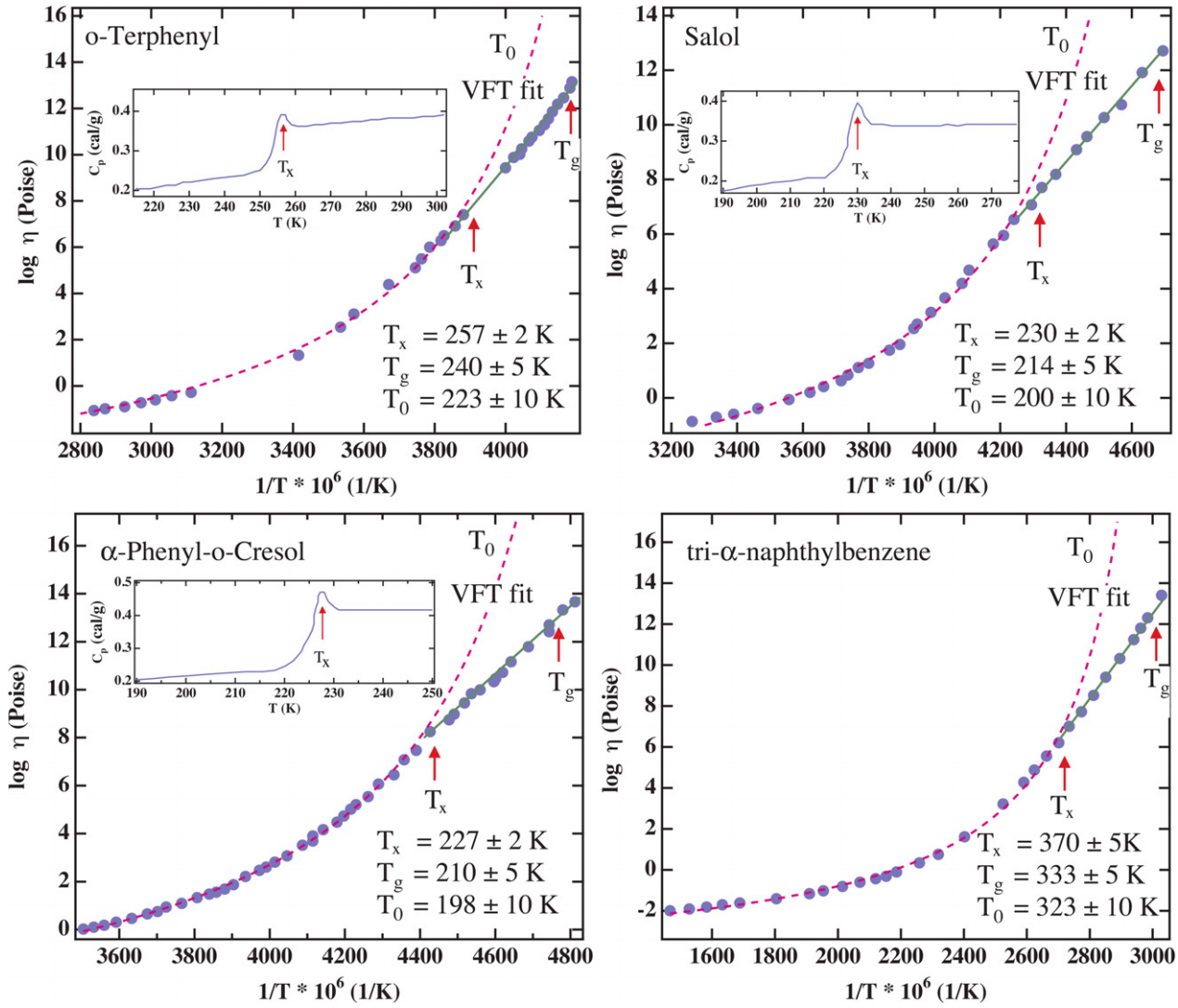

Figure 3. Evidence of the dynamic crossover phenomenon in the Arrhenius plot of the viscosity for four different well-known glass-forming liquids. (Top left) o-terphenyl; (top right) salol; (bottom left) alpha-phenyl-o-cresol; (bottom right) tri-alpha-naphtylbenzene. In the insets, we show their specific heat peaks at T_x [27]. We indicate these temperatures in the corresponding viscosity profiles with arrow signs at T_x. It should be noted that the arrows coincide with the turning point from a super-Arrhenius to an Arrhenius behavior in viscosity within the error bars. Specific heat data were not available for the case of tri-alpha-naphtylbenzene. The dotted pink lines represent the fit of the viscosity data with a VFT law at high temperatures; the green continuous lines are the fit with an Arrhenius law at low temperatures.

We calculated the self-intermediate scattering functions (ISF) for the oxygen atoms for five Q values (0.4, 0.5, 0.6, 0.7 and 0.8 Å^{-1}) and fit the data according to the RCM (top left panel). The top right and bottom right panels show the Arrhenius plots of the transport properties obtained from the trajectories: the translational relaxation time $\langle\tau\rangle$ and the inverse of the self-diffusion constant $1/D$, respectively. Both plots show a dynamic crossover at $T_L = 215 \pm 5$ K, analogous to the one in figure 1. As a side note, $\langle\tau(T_L)\rangle$ is between 1 and 10 ns for both experiments and simulations, confirming the general behavior of many glass formers [33].

The bottom left panel shows instead the dynamic response function $\chi_T(Q,t) = -\mathrm{d}F_s(Q,t)/\mathrm{d}T$ extracted from the trajectories. As also observed experimentally [16] the maximum of $\chi_T(Q,t)$, namely $\chi_T^*(Q)$, decreases after the dynamic crossover temperature $T_L = 215$ K. In conclusion, we showed that bulk water simulations are able to reproduce qualitatively our experimental findings of the 3D confined water in cement paste. The maximum of $\chi_T^*(Q)$ happens at the dynamic crossover temperature T_L and is not originated from the confinement.

In figure 6, we show a log–log plot of the self-diffusion constant extracted from the trajectories versus the translational relaxation time. The well-known Stokes–Einstein relation (SER) predicts a dependence $D \sim \tau^{-1}$. This is actually observed only at high temperatures, i.e. above T_L, while below the crossover temperature we observe a fractional dependence $D \sim \tau^{-0.92}$, close to the theoretical prediction of $D \sim \tau^{-2/2.1}$ for the three-dimensional strong liquid [34]. The emergence of the fractional SER starts at approximately $1.1T_L$. We have shown in 2006 [35] that the fractional SER appears also at $1.1T_L$ in the 1D confined water in MCM-41-S-15. In this

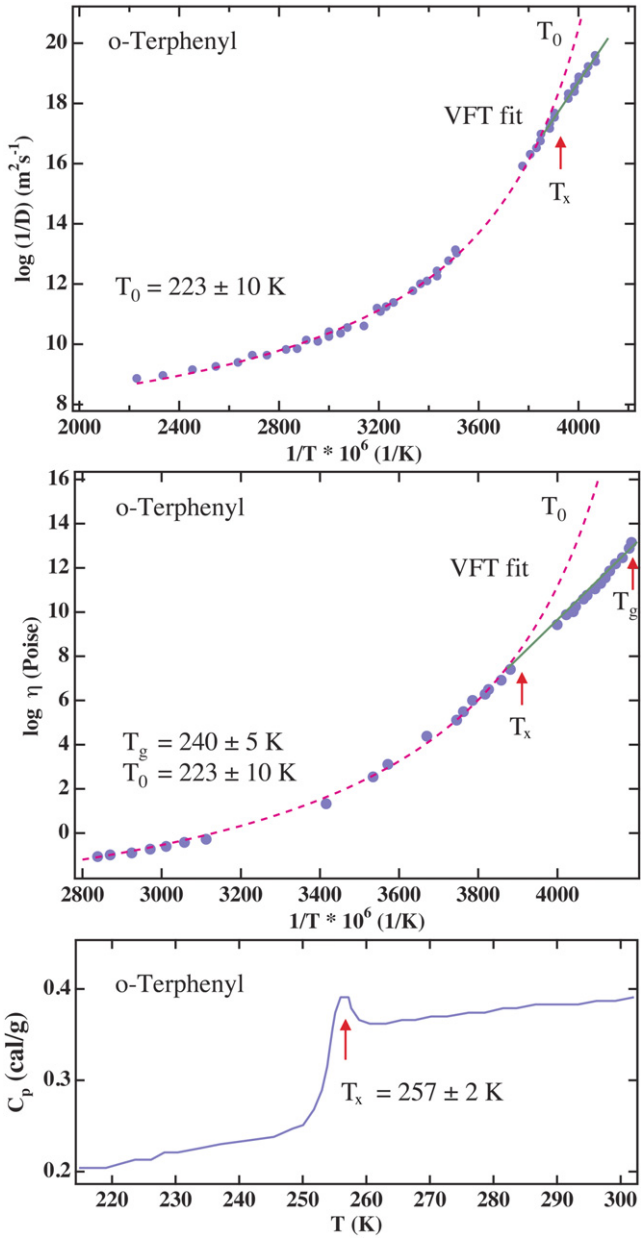

Figure 4. o-terphenyl dynamic crossover phenomenon. (Top) Arrhenius plot of the inverse of the self-diffusion constant; (middle) Arrhenius plot of the viscosity; (bottom) specific heat at constant pressure. The dotted pink lines represent the fit of the self-diffusion and viscosity data with a VFT law at high temperatures; the green continuous lines are the fit with an Arrhenius law at low temperatures. In each case, T_x is defined by the peak of the specific heat.

case, the exponent for the fractional SER has a value of 2/3, as predicted by the theory for the 1D case [34].

5. Predictions of the extended MCT

The idealized mode coupling theory [36] is the most successful microscopic theory for the glass transition. One of its major predictions is the existence of the critical temperature T_C at which the system undergoes an ergodic-to-nonergodic transition. T_C is a function of the so-called control variables which, in the case of the hard-sphere system, is the volume fraction of the hard spheres. In a system with a short-range attractive square-well potential besides the hard core, the control variables are the volume fraction and the scaled temperature $T^* = k_B T/\varepsilon$, where ε is the depth of the attractive square well (see a review [37]). Extensive tests of the theoretical predictions carried out so far against experimental data and computer simulation results suggest that the theory deals properly with some essential features of glass-forming liquids above T_C. On the other hand, a well-recognized limitation of the idealized MCT is the predicted divergence of the α relaxation time at the critical temperature T_C which is not observed in experiments and computer simulations. An extended version of MCT [38] aims at incorporating activated hopping processes which smear out the sharp nonergodic transition and restore ergodicity for $T < T_C$. But its applicability has been restricted to schematic models. In a new extended MCT (e-MCT) formulation for a Lennard-Jones system, Chong [39] treats hopping as arising from vibrational fluctuations in the quasi-arrested state where particles are trapped inside their cages. The resulting expression for the hopping rate takes an activated form, and the barrier height for the hopping is 'self-generated' in the sense that it is present only in those states where the dynamics exhibits a well-defined plateau.

This e-MCT predicts at T_C a dynamic crossover phenomenon instead of the real structural arrest transition [40]. In this section we would like to outline the predictions that this MCT makes, which are relevant to the interpretation of the phenomena we discussed above experimentally.

We show in figure 7 a series of self-intermediate scattering functions (ISF) of a Lennard-Jones system calculated by the e-MCT for different Q values and temperatures $\varepsilon = 1 - T/T_C$. It is visible from the figure that, at all temperatures, the calculated $F_s(Q,t)$ shows a two-step relaxation phenomenon where the short-time Gaussian-like relaxation is due to the vibrations of the typical Lennard-Jones particle trapped in the nearest-neighbor cage, and the long-time decay of the ISF can be represented well by a stretched exponential decay, representing the relaxation of the cage followed by the hopping of the trapped LJ particle. Moreover, from above T_C (negative ε) to below T_C (positive ε) the α relaxation time (defined by the relaxation time of the stretched exponential decay) progressively increases. A convenient way of determining the α relaxation time is by drawing a horizontal line at 0.1, and taking the intercept with $F_s(Q,t)$. The dimensionless Q value of 7.3 is the position where the first peak of the structure factor $S(Q)$ is located, while 10.0 is the position of the first minimum. So panel (a) represents the behavior of $F_s(Q,t)$ in the low-Q limit and panels (b) and (c) are the behavior of $F_s(Q,t)$ at the typical length scales in the Lennard-Jones liquid. It is obvious from the figure that there is no structural arrest at any temperature, especially at T_C ($\varepsilon = 0$ case), but instead there is a crossover phenomenon (see figure 11). In panel (d), we calculate the dynamic response function $\chi_T(Q,t) = -\mathrm{d}F_s(Q,t)/\mathrm{d}T$. The peak height of $\chi_T(Q,t)$, denoted as $\chi_T^*(Q)$, is related to the size of the dynamic heterogeneity in

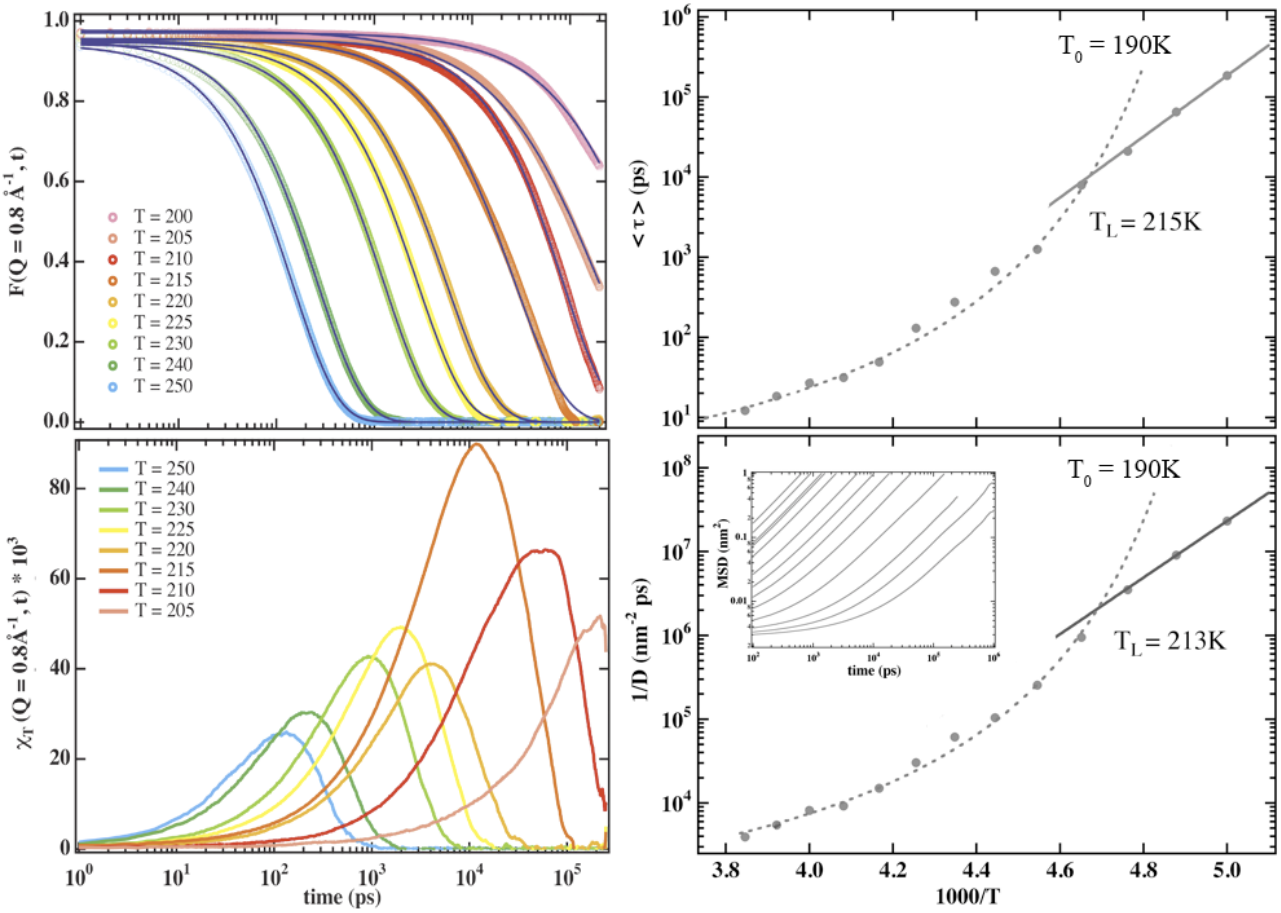

Figure 5. Numerical results from molecular dynamics simulations of bulk TIP4P-Ew water. (Top left) oxygen self-intermediate scattering functions at $Q = 0.8$ Å^{-1} for several temperatures. (Bottom left) dynamic response function, $\chi_T(Q, t)$, calculated with finite differences of the ISFs displayed in the top left panel. (Top right) Arrhenius plot of the α relaxation time, extracted by fitting the ISFs with the relaxing cage model. (Bottom right) Arrhenius plot of the inverse of the self-diffusion constant, extracted by fitting the mean square deviation (inset) with the Einstein relation.

the system [41, 16] and the peak position is approximately equal to the incoherent α relaxation time $\tau_{\rm inc}(Q, T)$ at that Q value. From the figure, it can be seen that its peak height $\chi_T^*(Q)$ increases as one approaches $T_{\rm C}$, but below $T_{\rm C}$ it decreases. We can attribute this to the existence of the crossover behavior (change of slope, $\mathrm{d}\log(\tau_{\rm i}(Q, T))/\mathrm{d}(1/T)$) in the Arrhenius plot of $\log(\tau_{\rm i}(Q, T))$ versus $1/T$ [16].

In figure 8 we want to check whether an analytical theory such as the e-MCT supports the relaxing cage model (RCM) that we used to analyze all our QENS spectra for confined water. According to this model, the incoherent self-intermediate scattering functions due to the hydrogen atoms in water are denoted by $F_H(Q, t)$ and are given by the following expression:

$$F_H(Q, t) = F^{\rm S}(Q, t) \exp\left[-\left(\frac{t}{\tau(Q, T)}\right)^{\beta}\right], \qquad (1)$$

where $F^S(Q, t)$ is the short-time vibrational motion of a typical water molecule in the cage formed by its immediate neighbor molecules. The second factor represents the long-time α relaxation of the cage. It is a stretched exponential form, containing a stretch exponent β, and the Q-dependent translational relaxation time $\tau(Q, T)$, which is a strong function of temperature. An essential assumption of the RCM is that $\tau(Q, T)$ takes a power law Q-dependent form such as $\tau_{\rm i}(Q, T) = \tau_0(T)(aQ)^{-\gamma}$, where a is the mean square vibrational amplitude of the molecule in the cage [23]. The Q-independent average translational relaxation time $\langle\tau\rangle$ is then evaluated as $\langle\tau\rangle = (\tau_0/\beta)\Gamma(1/\beta)$, where $\Gamma(x)$ is the gamma function. It essentially gives a measure of the structural relaxation time of the cage surrounding a typical molecule in the supercooled liquid. On the other hand, in the e-MCT the relaxation time $\tau(Q, T)$ represents the Q-dependent structural relaxation time of the cage surrounding a typical Lennard-Jones particle. In figure 8 we tested this power law Q dependence of the single-particle α relaxation time and it is obvious from the graph that, over the large Q-range, this power law Q dependence is valid also in e-MCT. We have shown before for the case of supercooled confined water in Vycor glass the validity of this power law dependence of the incoherent relaxation time experimentally [4].

In figure 9, we show the validity of the power law Q dependence for the coherent α relaxation time, which is given by $\tau_{\rm c}(Q, T) = \tau_1(T)(aQ)^{-\gamma} S(Q)$.

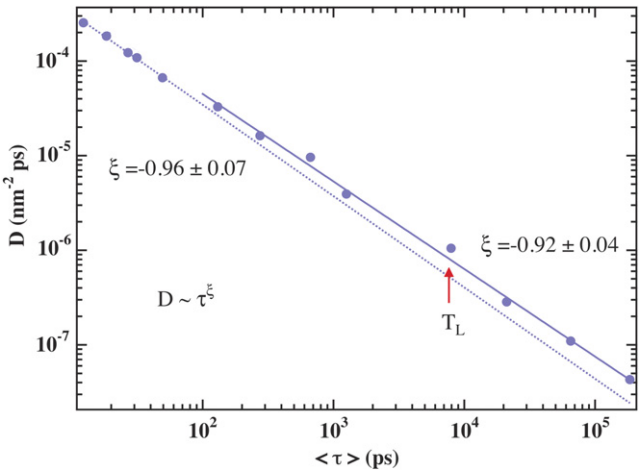

Figure 6. Log–log plot of D versus τ, showing the emergence of the fractional Stokes–Einstein relation (SER) below the crossover temperature for bulk TIP4P-Ew water. At temperatures 10% above T_L (indicated by the position of the red arrow) the exponent of the power law ξ is essentially unity, indicating the validity of the SER. Below T_L, the power law exponent switches to -0.92, close to the theoretical prediction of $-2/2.1$ within the error bars [34].

In figure 10, we show the temperature dependence of the power law exponent γ for both the coherent and the incoherent part. At high temperatures, the exponent γ in the incoherent case is 2, while the coherent case is 1. As the temperature is lowered below T_C, the two exponents merged into the same value of 1.5, indicating the strong coupling of the single-particle dynamics and the density fluctuations.

We now would like to ask a series of important questions: can the dynamic crossover phenomenon that we detected experimentally in all confined water be described as a fragile-to-strong dynamic crossover (FSC)? Specifically, do the single-particle and collective α relaxation times behave the same way as the shear viscosity as a function of temperature? If so, can the crossover temperature be identified as the T_C in the idealized mode coupling theory? We shall demonstrate in the next figure that answers to this series of questions are uniformly affirmative, at least for the Lennard-Jones system in e-MCT.

We show in figure 11 an Arrhenius plot of the three scaled quantities of the coherent and incoherent α relaxation times and the viscosity as a function of T_C/T, as predicted by the e-MCT. It is clearly visible in both panels that the behaviors of all three quantities are very close to each other, at least in the vicinity of the MCT T_C. Furthermore, the crossover temperature is best identified to be at T_C and for practical purposes the maximum slope in the Arrhenius plot of the viscosity (bottom panel) can be used to detect the position of the crossover temperature, as was already demonstrated in figure 1. An alternative way of determining the crossover temperature is through the plot of the dynamic response function $\chi_T(Q,t)$ as a function of time for a series of temperatures and to choose the temperature where the peak height $\chi_T^*(Q)$ is maximum, as was shown in panel (d) of figure 7.

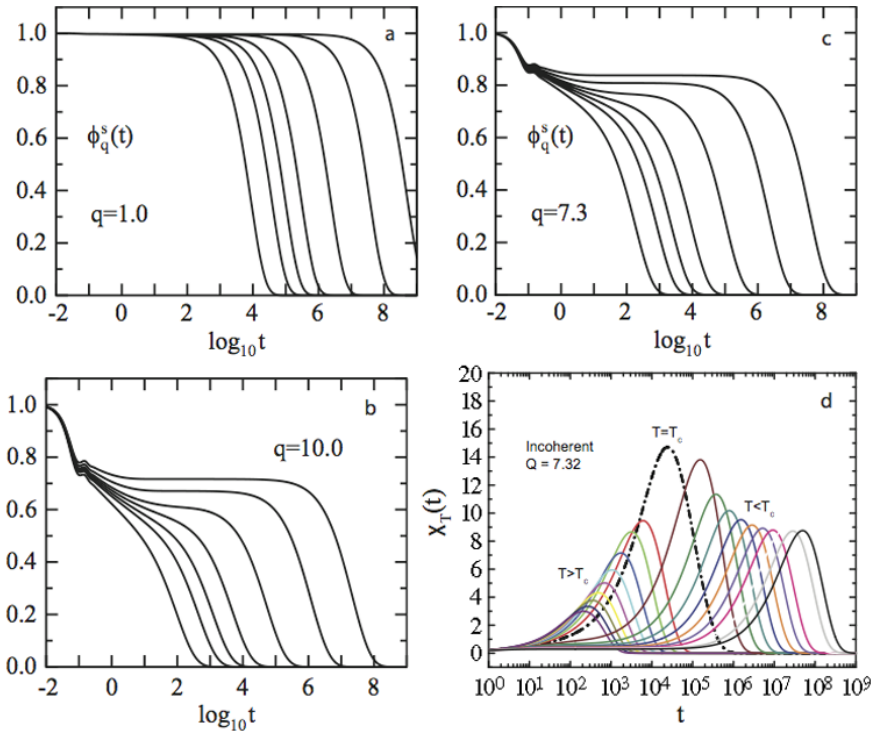

Figure 7. Predictions of the e-MCT for a Lennard-Jones system. (a)–(c) Self-intermediate scattering functions at $q = 1.0$, 7.3 and 10.0 (in a reduced unit), respectively, for $\varepsilon = 1 - T/T_C = -0.10$, -0.05, -0.03, -0.01, 0.01, 0.05 and 0.10 from left to right. $q = 7.3$ corresponds to the first peak in the structure factor, while $q = 10.0$ is the first minimum. (d) Dynamic response function, $\chi_T(q,t)$, for $q = 7.3$. The peak height, $\chi_T^*(Q)$, increases towards T_C and decreases after, as observed in the experiments of confined water [16] and the MD simulations of bulk water (figure 5).

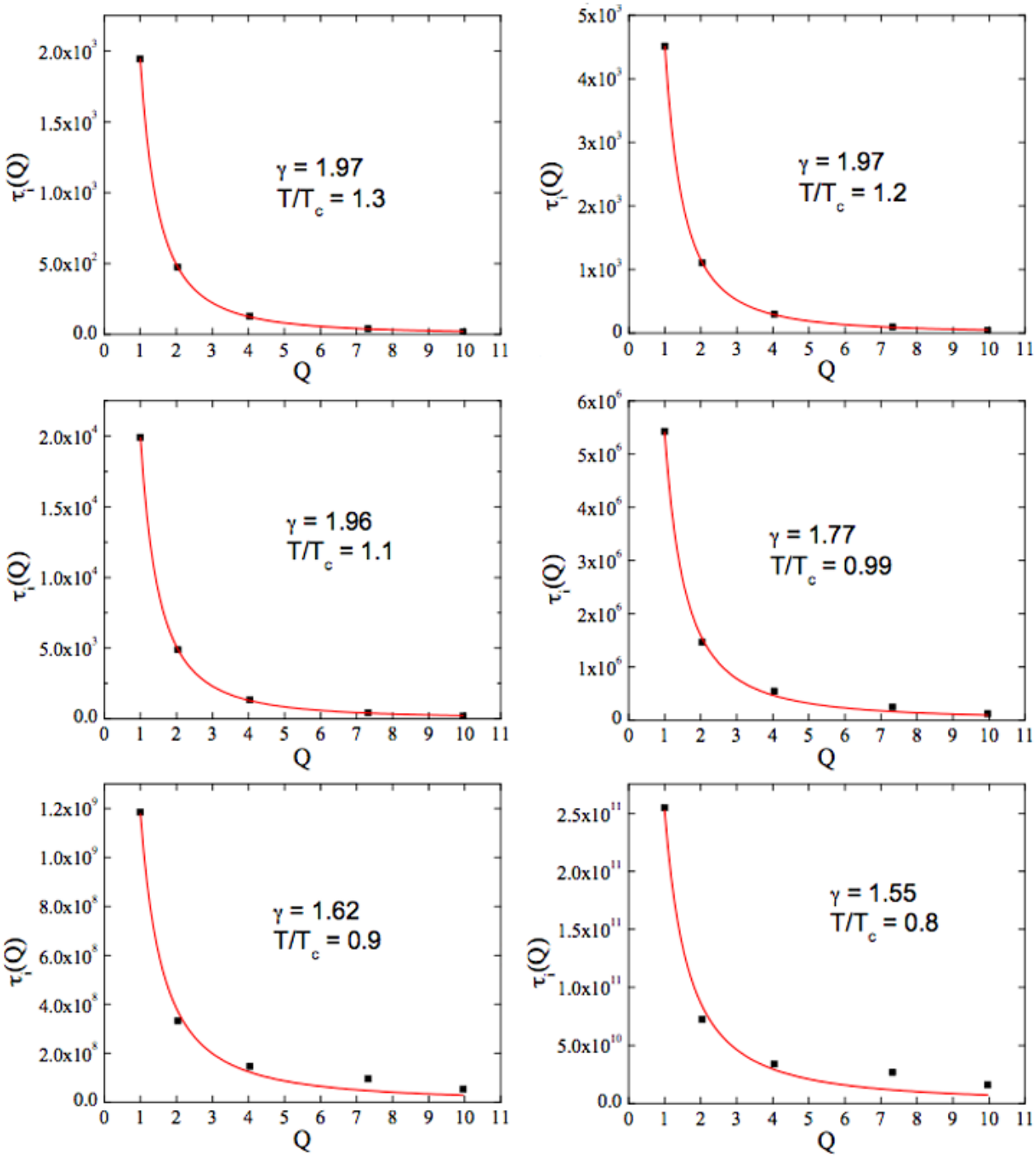

Figure 8. Predictions of the e-MCT. The black dots are the incoherent α relaxation times $\tau_i(Q, T)$ calculated from e-MCT for a series of temperatures. The red lines are the best fits to the Q dependence of the incoherent α relaxation time with the power law expression contained in the relaxing cage model (RCM) [22, 23]: $\tau_i(Q, T) = \tau_0(T)(aQ)^{-\gamma}$.

6. Concluding remarks

In this paper, we begin by experimentally showing clear evidence of the existence of a super-Arrhenius (fragile) to Arrhenius (strong) dynamic crossover (FSC) both in supercooled confined water and in common glass-forming liquids. The dynamic crossover temperature in MD simulation of bulk water $T_L = 215$ K is about 13% higher than $T_g \approx T_0 = 190$ K. The dynamic crossover temperature we defined as T_x in other organic liquids is about 7% higher than the calorimetric glass transition temperature T_g. As a result, we can state that classifying a glass-forming liquid as either a 'fragile' or a 'strong' liquid is only an approximate concept valid only in a limited range of temperatures for each glass-forming liquid. There is overwhelming experimental evidence [26] that every liquid would become 'strong' at sufficiently low temperatures

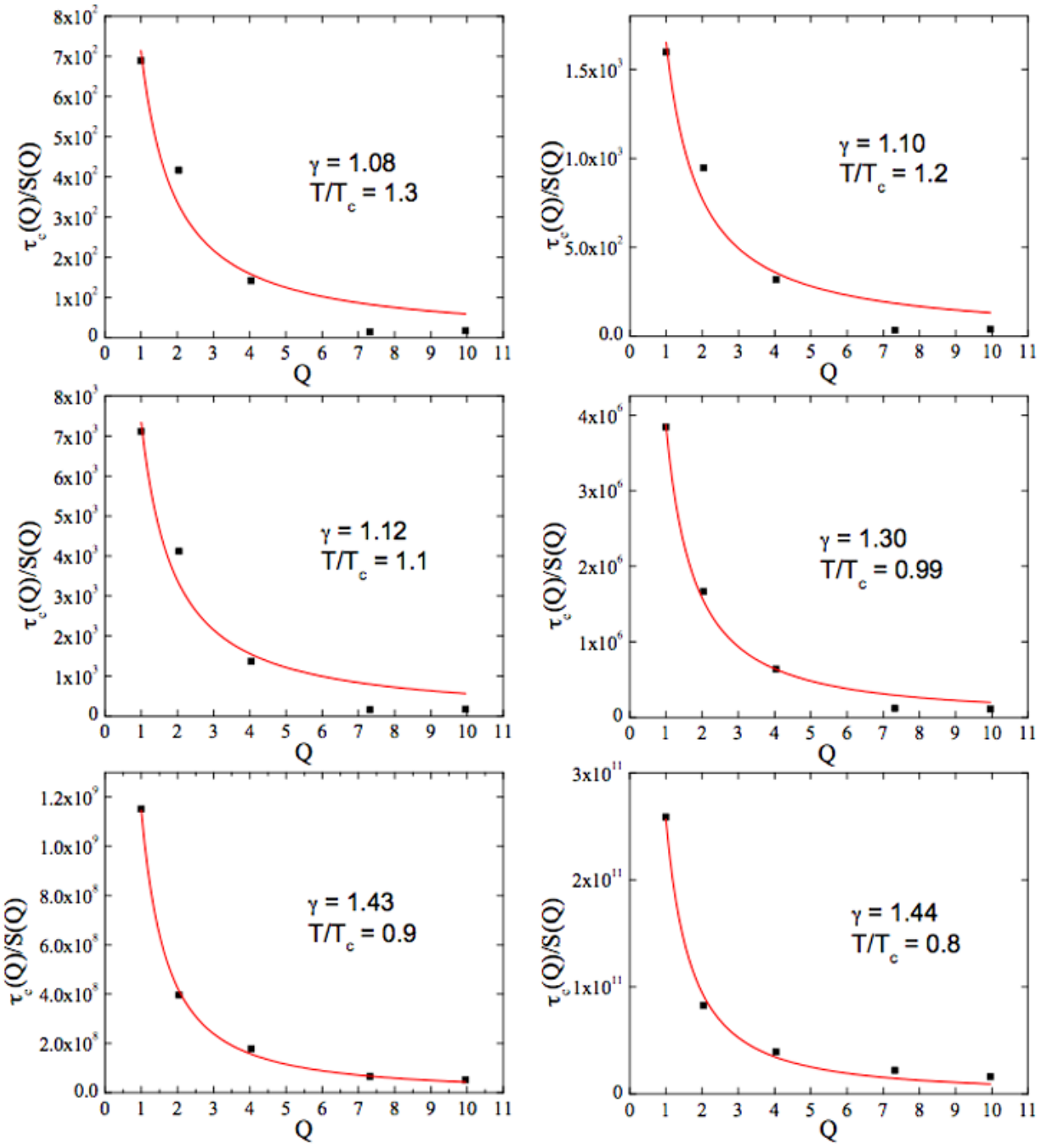

Figure 9. Predictions of the e-MCT. The black dots are the coherent α relaxation times $\tau_c(Q, T)$ calculated from e-MCT for a series of temperatures. The red lines are the best fits to the Q dependence of the coherent α relaxation time with the power law expression $\tau_c(Q, T) = \tau_1(T)(aQ)^{-\gamma} S(Q)$.

before the glass transition temperature. However, we are not certain at this time whether we can identify the crossover temperature T_x as the mode coupling T_c other than that in the case of the Lennard-Jones system, since in the literature there are reports of the determination of T_c [33] in the liquids we presented in figures 3 and 4. The two most convenient ways of detecting the crossover temperature are (1) taking the derivative of the Arrhenius plot of the transport properties and locating the temperature where the slope is maximum or (2) plotting the dynamic response function as a function of time for several temperatures and taking the temperature where its peak height becomes maximum.

Molecular dynamics simulations on bulk water show that the FSC observed experimentally in supercooled confined water is not due to the confinement. Moreover, below T_L the fractional Stokes–Einstein relation emerges. It has been shown by Mazza *et al* [44] by an MD simulation that the Debye–Stokes–Einstein relation also breaks down in the vicinity of T_L

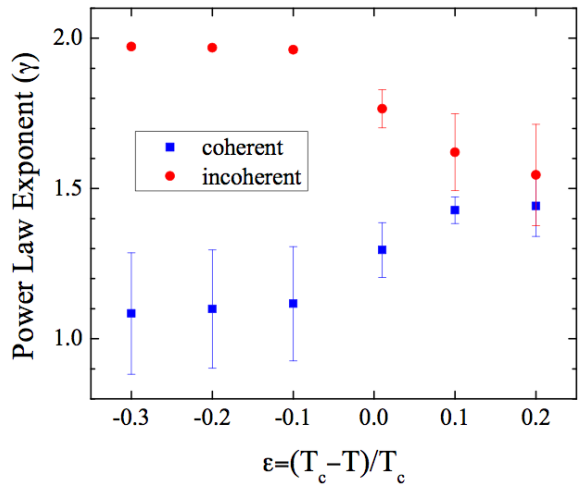

Figure 10. The power law exponents of the coherent and incoherent α relaxation times as a function of $\varepsilon = 1 - T/T_C$. Asymptotically, the exponents of the power law Q dependence of $\tau_i(Q)$ and $\tau_c(Q)$ become the same $\gamma_i = \gamma_c = 1.5$ at low temperatures, providing evidence of the strong coupling between self-and collective motions below T_c.

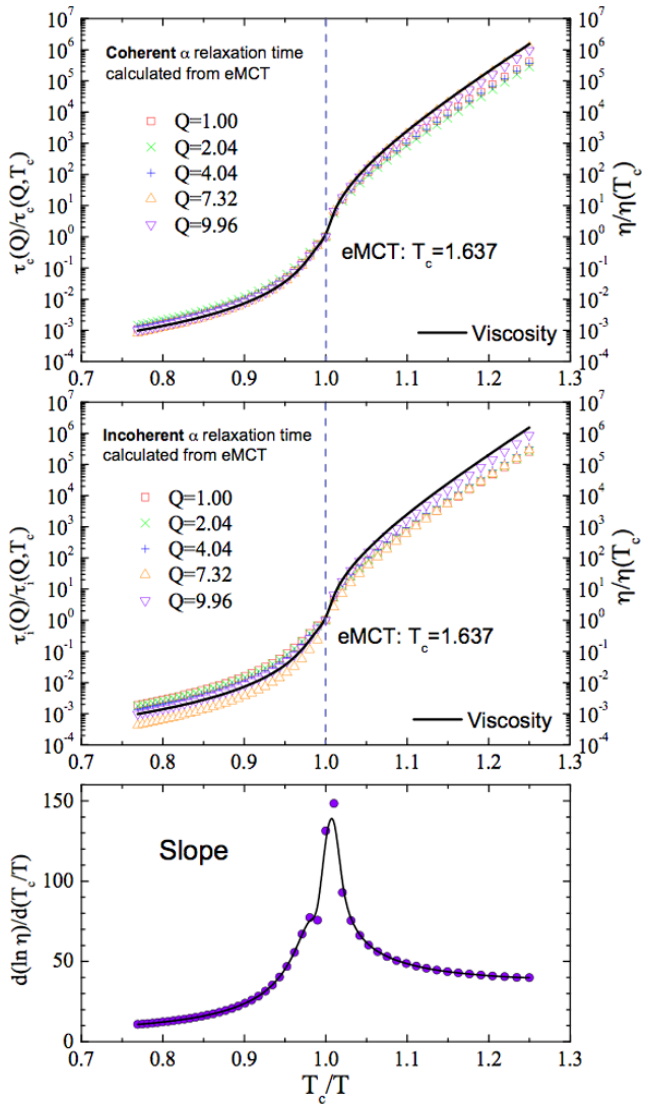

Figure 11. Top and middle panels: scaling plot of $\tau(Q)/\tau(Q, T_c)$ and $\eta/\eta(T_c)$ versus T_c/T of the normalized α relaxation time $\tau_{coh}(Q)$, $\tau_{inc}(Q)$ and viscosity calculated from the e-MCT. When their Q dependence is scaled out in this way, the coherent and incoherent α relaxation times and the viscosity behave essentially the same way, showing a similar crossover phenomenon. Bottom panel: the slope in the Arrhenius plot of the viscosity shows a sharp peak at T_c. Therefore it is reasonable to locate the T_c by the peak position of the maximum slope in the Arrhenius plot of the viscosity.

of bulk SPC-E water [45]. Furthermore, a well-defined boson peak in the incoherent inelastic neutron scattering spectrum begins to appear, as shown in figure 12 for the case of confined water in an aged cement paste. The peak appears between 240 and 220 K, in the range of temperatures where we demonstrated that the dynamic crossover phenomenon takes place in figure 1.

In the case of water, the crossover phenomenon seems to be a result of the existence of a peak in the specific heat which is located exactly at this crossover temperature (as seen in figures 1 and 2). The origin of this peak in the specific heat can be attributed in this case to the crossing of the Widom line in the one-phase region [42], derived from the hypothetical existence of a liquid–liquid critical point at an elevated pressure [7].

An extended mode coupling theory of the Lennard-Jones system predicts that the FSC temperature T_L of viscosity and α relaxation times coincides with the mode coupling T_C. Thus the dynamic crossover phenomenon in a common glass-forming liquid can be attributed to a change of dynamic behavior of the supercooled liquid from a regime dominated by the caging effect in a dense liquid to a quasi-arrested regime where the relaxation is only possible with the help of collective hopping processes (dynamic heterogeneities).

In conclusion, we would like to stress that, from a physical point of view, a genuine change of thermodynamic and dynamic behavior is taking place at T_L and T_x, not at the traditionally emphasized T_g. In the supercooled glassy liquids, the thermodynamics and the dynamics are mutually coupled through the Adam–Gibbs relation [24].

Acknowledgments

Research at MIT is supported by DE-FG02-90ER45429; at the University of Florence by MIUR and CSGI; at the Institute for Molecular Science in Japan by Grants-in-Aid for scientific research from the Ministry of Education, Culture, Sports, Science and Technology of Japan (no. 20740245). The neutron scattering experiment is done at the Spallation Neutron Source at Oak Ridge National Laboratory. The facility was sponsored by the Scientific User Facilities Division, Office of Basic Energy Sciences, US Department of Energy. We benefited from affiliation with the European Union-Marie Curie Research and Training Network on Arrested Matter. We would like to thank Eugene Mamontov for assistance at the BASIS experiments and John Copley for the measurement at DSC of NIST NCNR. This work utilized facilities supported

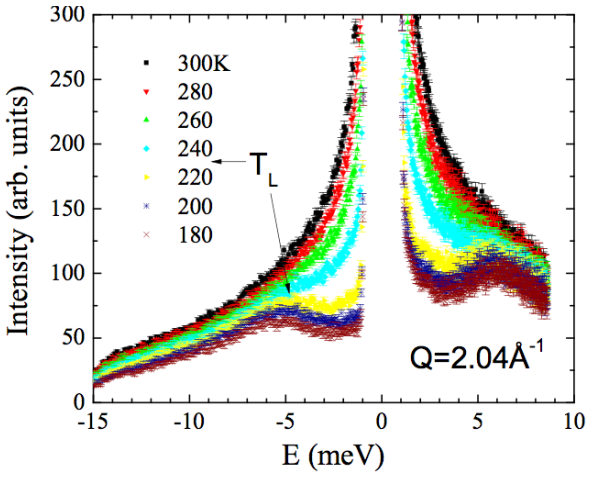

Figure 12. Inelastic neutron scattering spectra of 3D confined water measured from 300 down to 180 K in steps of 20 K. A well-defined boson peak at about 5 meV starts building up below the dynamic crossover temperature $T_L = 230 \pm 10$ K (between the curves with circle and diamond symbols).

in part by the National Science Foundation under agreement no. DMR-0454672.

References

[1] Debenedetti P G 2003 *J. Phys.: Condens. Matter* **15** R1669–726
[2] Ball P 2008 *Nature* **452** 291
[3] Webber B and Dore J 2004 *J. Phys.: Condens. Matter* **16** S5449–70
[4] Zanotti J M, Bellissent-Funel M-C and Chen S-H 1999 *Phys. Rev.* E **59** 3084
[5] Takahara S, Nakano M, Kittaka S, Kuroda Y, Mori T, Hamano H and Yamaguchi T 1999 *J. Phys. Chem.* B **103** 5814
[6] Faraone A, Liu L, Mou C-Y, Yen C-W and Chen S-H 2004 *J. Chem. Phys.* **121** 10843
[7] Liu L, Chen S-H, Faraone A, Yen C-W and Mou C-Y 2005 *Phys. Rev. Lett.* **95** 117802
[8] Swenson J, Jansson H, Howells W S and Longeville S 2005 *J. Chem. Phys.* **122** 084505
[9] Yoshida K, Yamaguchi T, Kittaka S, Bellissent-Funel M-C and Fouquet P 2008 *J. Chem. Phys.* **129** 054702
[10] Angell C A 2004 *Annu. Rev. Phys. Chem.* **55** 559–83
[11] Poole P, Sciortino F, Essmann U and Stanley H E 1992 Phase behavior of metastable water *Nature* **360** 324
[12] Mamontov E 2005 *J. Chem. Phys.* **123** 171101
Mamontov E 2006 *J. Chem. Phys.* **124** 194703
[13] Chen S-H, Liu L, Fratini E, Baglioni P, Faraone A and Mamontov E 2006 *Proc. Natl Acad. Sci. USA* **103** 9012
[14] Chen S-H, Liu L, Chu X, Zhang Y, Fratini E, Baglioni P, Faraone A and Mamontov E 2006 *J. Chem. Phys.* **125** 171103
[15] Chu X, Fratini E, Baglioni P, Faraone A and Chen S-H 2008 *Phys. Rev.* E **77** 011908
[16] Zhang Y *et al* 2008 *J. Phys.: Condens. Matter* **20** 502101
Zhang Y, Lagi M, Fratini E, Baglioni P, Mamontov E and Chen S-H 2009 *Phys. Rev.* E **79** 040201(R)
[17] Kolesnikov A I, Zanotti J-M, Loong C-K, Thiyagarajan P, Moravsky A P, Loutfy R O and Burnham C J 2004 *Phys. Rev. Lett.* **93** 035503
[18] Mamontov E, Burnham C J, Chen S-H, Moravsky A P, Loong C-K, de Souza N R and Kolesnikov A I 2006 *J. Chem. Phys.* **124** 194703
[19] Chu X-Q, Kolesnikov A I, Moravsky A P, Garcia-Sakai V and Chen S-H 2007 *Phys. Rev.* E **76** 021505
[20] Jennings H M 2008 *Cem. Concr. Res.* **38** 275
[21] Ridi F, Luciani P, Fratini E and Baglioni P 2009 *J. Phys. Chem.* B **113** 3080
[22] Chen S H *et al* 1999 *Phys. Rev.* E **59** 6708
[23] Liu L *et al* 2004 *J. Phys.: Condens. Matter* **16** S5403
Liu L, Chen S-H, Faraone A, Yen C-W, Mou C-Y, Kolesnikov A, Mamontov E and Leao J 2006 *J. Phys.: Condens. Matter* **18** S2261–84
[24] Adam G and Gibbs J H 1965 *J. Chem. Phys.* **43** 139
[25] Maruyama S, Wakabayashi K and Oguni M 2004 Thermal properties of supercooled water confined within silica gel pores *Slow Dynamics in Complex Systems: 3rd Int. Symp.* ed M Tokuyama and I Oppenheim
[26] Mallamace F, Branca C, Corsaro C, Leone N, Spooren J, Chen S-H and Stanley H E, Experimental evidence for fragile to strong crossover in general glass forming liquids, at press
[27] Laughlin W T and Uhlmann D R 1972 *J. Phys. Chem.* **76** 2317
[28] Mapes M K, Swalln S F and Ediger M D 2006 *J. Phys. Chem.* B **110** 507
[29] Horn H W *et al* 2004 *J. Chem. Phys.* **120** 9665
[30] Xu L-M *et al* 2005 *Proc. Natl Acad. Sci. USA* **102** 16558
[31] Kumar P *et al* 2008 *Phys. Rev. Lett.* **100** 105701
[32] Sciortino F *et al* 1996 *Phys. Rev.* E **54** 6331
[33] Novikov V N and Sokolov A P 2003 *Phys. Rev.* E **67** 031507
[34] Jung Y J, Garrahan J P and Chandler D 2005 *J. Chem. Phys.* **123** 084509
[35] Chen S-H, Mallamace F, Mou C-Y, Broccio M, Corsaro C, Faraone A and Liu L 2006 *Proc. Natl Acad. Sci. USA* **103** 12974–8
[36] Götze W 1991 *Liquids, Freezing and Glass Transition* ed J-P Hansen, D Levesque and J Zinn-Justin (Amsterdam: North-Holland) p 287
[37] Sciortino F and Tartaglia P 2005 *Adv. Phys.* **54** 471
[38] Götze W and Sjögren L 1987 *Z. Phys.* B **65** 415
[39] Chong S H 2008 *Phys. Rev.* E **78** 041501
[40] Chong S H 2009 A possible scenario for the fragile-to-strong dynamic crossover predicted by the extended mode-coupling theory for glass transition *J. Phys.: Condens. Matter* **21** at press
[41] Berthier L *et al* 2005 *Science* **310** 1797
[42] Xu L, Kumar P, Buldyrev S V, Chen S H, Poole P H, Sciortino F and Stanley H E 2005 *Proc. Natl Acad. Sci. USA* **102** 16558–62
[43] Kumar P, Yan Z, Xu L, Mazza M G, Buldyrev S V, Chen S-H, Sastry S and Stanley H E 2006 *Phys. Rev. Lett.* **97** 177802–6
[44] Mazza M G, Giovambattista N, Stanley H E and Starr F W 2007 *Phys. Rev.* E **76** 031203
[45] Starr F W, Sciortino F and Stanley H E 1999 *Phys. Rev.* E **60** 6757